An Input-Oriented Power Sharing Control Scheme With Fast-Dynamic Response for ISOP DAB DC–DC Converter

Nie Hou, *Student Member, IEEE*, Pasan Gunawardena, *Student Member, IEEE*, Xuesong Wu, *Student Member, IEEE*, Li Ding, *Member, IEEE*, Yue Zhang, *Member, IEEE*, and Yun Wei Li, *Fellow, IEEE*

***Abstract*—With some advantages, such as electric isolation, high efficiency, and fast dynamic response, the input-series output-parallel (ISOP) dual-active-bridge (DAB) dc–dc converter has been regarded as one of the most promising candidates for connecting the medium voltage terminal and the low voltage terminal. For the ISOP DAB dc–dc converter, the existing control strategies are mainly focusing on the equivalent power sharing control, but the fast-dynamic response is not included and the decoupling between the regulation of input voltage and the adjustment of output voltage is not eliminated significantly. In this article, the average model of this ISOP DAB dc–dc converter is presented first, which can be employed to analyze the power distributions of this modular topology clearly. Then, an input-oriented power sharing control scheme with fast-dynamic response is proposed for ensuring both the power sharing ability and the fast-dynamic performance of the ISOP DAB dc–dc converter in this article. Compared with the existing methods, this proposed scheme can also significantly reduce the coupling between the power sharing control and the output voltage regulation. In addition, an inductance-estimating method is proposed for ensuring the power sharing performance of the ISOP DAB dc–dc converter. Finally, the experimental results are provided to verify the effectiveness of the proposed input-oriented power sharing control with fast-dynamic response for the ISOP DAB dc–dc converter system.**

***Index Terms*—Average model, fast-dynamic response, input-series output-parallel (ISOP) dual-active-bridge (DAB) converter, power balancing control.**

I. Introduction

HIGH-VOLTAGE dc converter systems with large voltage turn ratio are extensively used in some power electronic applications, such as rail transit system, energy storage system, and microgrids [1]–[5]. Then, based on input-series output-parallel (ISOP) structure, the power electronic transformers with electric isolation become a promising candidate for connecting the medium/high voltage dc and the low voltage dc in these converteryy systems [6], [7]. Generally, compared with other isolated dc–dc converters, the dual-active-bridge (DAB) is more suitable for high power applications with high efficiency, bidirectional operation, and fault isolation [8], [9]. So, this article mainly focuses on the ISOP DAB dc–dc converter as shown in Fig. 1 for uninterrupted power supply.

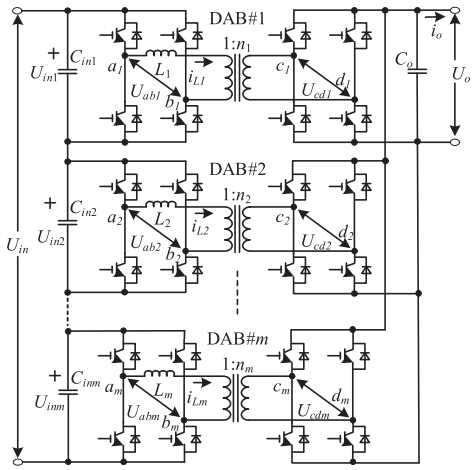

Fig. 1. Topology of the ISOP DAB dc–dc converter system.

With equivalent power sharing control for ISOP converter system, the equivalent utilization of components can be ensured, and the overvoltage overcurrent issues can be avoided for each converter module [10]. Traditionally, the common duty-ratio operation can be employed to realize power balance performance in parallel/series dc–dc converter system [11], [12], which can significantly reduce the design cost of the controller system. However, the power balance performance is sensitive to the parameter mismatch, especially for the DAB type converter, and the transient process may result in instability under common duty ratio control [13], [14].

To realize positive power sharing control operation, there are two main ways to realize the power balance control for

Manuscript received July 8, 2021; revised September 30, 2021 and November 9, 2021; accepted December 17, 2021. Date of publication December 24, 2021; date of current version February 18, 2022. This work was supported in part by the Future Energy Systems initiative funding from the Canada First Research Excellence Fund and in part by the Alberta Innovates Graduate Student Scholarship from the Alberta Innovates. Recommended for publication by Associate Editor F. J. Azcondo. *(Corresponding author: Yue Zhang.)*

The authors are with the Department of Electrical and Computer Engineering, University of Alberta, Edmonton, AB T6G 2V4, Canada (e-mail: nhou@ualberta.ca; pasan@ualberta.ca; xuesong3@ualberta.ca; lding@ualberta.ca; yue30@ualberta.ca; yunwei.li@ualberta.ca).

Color versions of one or more figures in this article are available at https://doi.org/10.1109/TPEL.2021.3138126.

Digital Object Identifier 10.1109/TPEL.2021.3138126

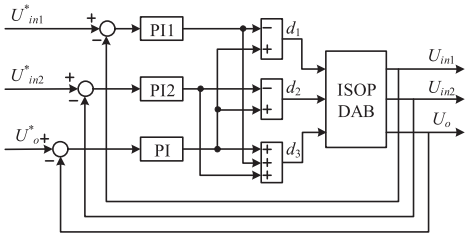

Fig. 2. Traditional decoupling compensation structure for the ISOP DAB dc–dc converter system with three modules [26], [27].

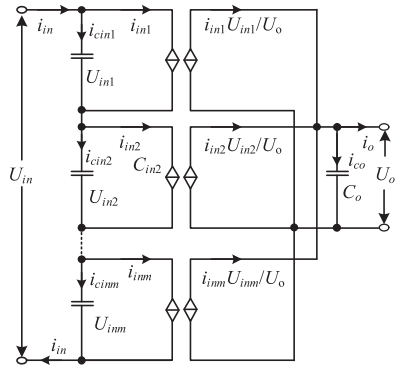

Fig. 3. Simplified circuit of the ISOP DAB dc–dc converter system.

the ISOP dc–dc converter including the positive input-voltage control scheme [15]–[18] and the positive transferred-current control scheme [19]–[23]. For the positive input-voltage control scheme, these existing control strategies can be divided into two groups including the input voltage direct control [15], [16] and the input-voltage droop control [17], [18]. Moreover, for the positive transferred-current control scheme, there are also two categories including the transferred-current direct control [19] and the transferred-current droop control [22], [23]. In [15], a simple sensorless current mode control scheme is proposed for guaranteeing stable sharing performance of the ISOP dc–dc converter system. Similarly, based on the same outer control structure, an input voltage sharing control method is proposed for the ISOP forward dc–dc converter system [16], and the equivalent input voltages can be obtained. For modular converter systems, the droop control concept is also a potential candidate for realizing the power balance performance. Based on the droop structure, a wireless input voltage sharing control method is proposed for the isolated dc–dc converter [17], and a similar decentralized control method is proposed for ISOP DAB dc–dc converter system. Moreover, by directly controlling the transferred current, the power balance operation can be realized, but the converter system prefers to be unstable with the negative resistance model [24]. So, a transferred-current differential control scheme is proposed to address this issue [19]. Furthermore, the transferred-current droop control method can be employed to achieve the power balance control for the ISOP dc–dc converter [22]. A decentralized inverse-droop control method is proposed for balancing power sharing of the ISOP isolated dc–dc converter [23].

Since the transferred current of the DAB dc–dc converter contains the ac current, the transferred-current-based control should be not suitable. Moreover, the droop-based control scheme usually results in poor dynamic and steady-state performances [25]. So, the input-voltage direct control may be the most suitable control for the ISOP DAB dc–dc converter [15], [16], but the decoupling between the regulation of input voltage and the adjustment of output voltage in the traditional ways may result in a bad transient process. So, a novel input voltage sharing control is proposed to decouple the input voltage with the output voltage regulation as shown in Fig. 2 [26], [27]. However, since the PI controller for adjusting the input voltage of the first two modules is employed to determine the phase-shift ratio not the transferred power, the influence on the output voltage is also obvious. In addition, these existing strategies are more focusing on the power sharing performance, and the fast-dynamic response for the ISOP DAB dc–dc converter is not studied for dealing with the disturbances of the input voltage and the load current.

Therefore, a novel input-oriented power sharing control method with fast-dynamic response is proposed for the ISOP DAB dc–dc converter system in this article, which can be employed to adjust the input voltages of different modules flexibly for required power sharing performance and maintain the output voltage when the input voltage and load resistor are changed.

The rest of this article is organized as follows. The average model of this ISOP DAB dc–dc converter is demonstrated in Section II. Then, in Section III, combining a minimum-current-stress (MCS) modulation method, the novel power sharing control scheme with fast-dynamic response is proposed. Moreover, an inductance-estimating method is proposed for ensuring the power sharing performance of the ISOP DAB dc–dc converter. In addition, based on experimental results, the effectiveness of the proposed input-oriented power sharing control scheme with fast-dynamic response is verified in Section IV. Finally, Section V concludes this article.

II. Average Model of the ISOP DAB DC–DC Converter System

In this section, the average model of the ISOP DAB dc–dc converter system as shown in Fig. 1 will be presented. Then, the current distributions on both the primary side and the secondary side will be demonstrated, which can be employed to analyze the coupling relationship between the adjustment of the input voltages and the output voltage.

A. Average Model of the ISOP DAB DC–DC Converter

Traditionally, the inductance of the dc–dc converter, such as buck converter and boost converter plays an important role in the modeling analysis. Nevertheless, since the transferred current of the DAB dc–dc converter can be determined by the circuit parameter and the phase-shift ratio, the middle ac inductance can be neglectful [28], [29]. Then, the simplified circuit of the ISOP DAB dc–dc converter system can be shown in Fig. 3, where the input-side current and the output-side current can be modeled as controllable current source.

According to Fig. 3, the average model of the ISOP DAB dc–dc converter can be expressed as

$$\begin{cases} C_{\text{in}X}\frac{dU_{\text{in}X}}{dt} = i_{\text{in}} - i_{\text{in}X} \\ C_o\frac{dU_o}{dt} = \sum_{\alpha=1}^{m}\frac{i_{\text{in}X}U_{\text{in}X}}{U_o} - i_o \end{cases} \quad (X \in [1,m]). \tag{1}$$

Then, the small-signal model of this ISOP DAB dc–dc converter can be expressed as

$$\begin{cases} C_{\text{in}X}\frac{d\hat{U}_{\text{in}X}}{dt} = \hat{i}_{\text{in}} - \hat{i}_{\text{in}X} \\ C_o\frac{d\hat{U}_o}{dt} = \sum_{X=1}^{m}\frac{\hat{i}_{\text{in}X}U_{\text{in}X}}{U_o} + \sum_{X=1}^{m}\frac{i_{\text{in}X}\hat{U}_{\text{in}X}}{U_o} - \hat{i}_o \end{cases} \quad (X \in [1,m]). \tag{2}$$

According to (1), since the total disturbances of the input voltage for each DAB module should be zero, the input current i_{in} can be expressed as

$$i_{\text{in}} = \frac{\sum_{X=1}^{m}\frac{i_{\text{in}X}}{C_{\text{in}X}}}{\sum_{X=1}^{m}\frac{1}{C_{\text{in}X}}} = \frac{\sum_{X=1}^{m} i_{\text{in}X}}{m}\Big|_{\text{same input capacitors}}. \tag{3}$$

In (3), when the ISOP DAB dc–dc converter is at steady-state condition, the transferred current for each DAB module $i_{\text{in}X}$ should be equivalent to the input current i_{in}.

B. Inherent Coupling Phenomenon Between Regulations of Input Voltages and Output Voltage

Then, assuming the input capacitors are the same, when a variation $\Delta i_{\text{in}H}$ is added to the Hth DAB module for adjusting its input voltage, the input voltage i_{in} can be expressed as

$$i_{in} = \frac{\sum_{X=1}^{m} i_{\text{in}X} + \Delta i_{\text{in}H}}{m} = i'_{\text{in}} + \frac{\Delta i_{\text{in}H}}{m}. \tag{4}$$

where i'_{in} is the required input current for the load side at steady-state condition. Then, the capacitor charging current $i_{\text{cin}X}$ for each DAB module can be expressed as

$$\begin{cases} i_{\text{cin}H} = -\frac{m-1}{m}\Delta i_{\text{cin}H} \\ i_{\text{cin}X} = \frac{1}{m}\Delta i_{\text{cin}H} \end{cases} \quad (X \neq H). \tag{5}$$

On this condition, the transferred current to the output side can be calculated as

$$\begin{aligned} \sum_{X=1}^{m}\frac{i_{\text{in}X}U_{\text{in}X}}{U_o} &= \sum_{X=1}^{m}\frac{i'_{\text{in}}U_{\text{in}X}}{U_o} + \frac{\Delta i_{\text{in}H}U_{\text{in}H}}{U_o} \\ &= U_o i_o + \frac{\Delta i_{\text{in}H}U_{\text{in}H}}{U_o}. \end{aligned} \tag{6}$$

According to (6), the charging current of the output capacitor i_{co} can be calculated as

$$i_{co} = \frac{\Delta i_{\text{in}H}U_{\text{in}H}}{U_o}. \tag{7}$$

Then, the output voltage will be not stable since the charging current of the output capacitor is not zero. Moreover, when all input voltages $U_{\text{in}X}$ should be adjusted positively for the desired power sharing performance, the variation $\Delta i_{\text{in}X}$ for each DAB module can be expressed as

$$\Delta i_{\text{in}X} = C_X\Delta U_{\text{in}X} \quad \left(\sum_{X=1}^{m}\Delta U_{\text{in}X} = 0\right). \tag{8}$$

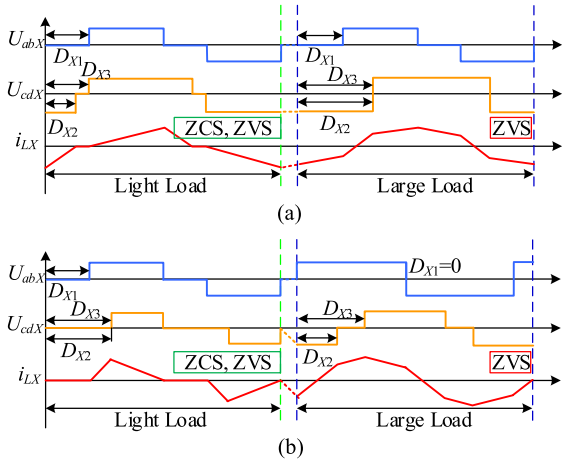

Fig. 4. MCS modulation method under different voltage conditions. (a) Phase-shift modulation methods when $k > 1$. (b) Phase-shift modulation methods when $k > 1$.

Assuming the input capacitors are the same, the sum of the transferred current variations can be expressed as

$$\sum_{X=1}^{m}\Delta i_{\text{in}X} = 0. \tag{9}$$

According to (3) and (9), the input current i_{in} will not be changed. Then, combining Fig. 3 and (6), the charging current i_{co} of the output capacitor can be expressed as

$$i_{co} = \sum_{X=1}^{m}\frac{\Delta i_{\text{in}X}U_{\text{in}X}}{U_o} \neq 0 \qquad \left(\sum_{X=1}^{m}\Delta i_{\text{in}X} = 0\right). \tag{10}$$

During the transient process for adjusting the input voltages, the input voltages $U_{\text{in}X}$ for each DAB module are usually not the same, so the charging current for the output capacitor is not zero. Then, the disturbance of the output voltage is not evitable. In reverse, if i_{co} is forced to zero in (10), the disturbance of the output voltage can be omitted, but the sum of the transferred current variations cannot be zero. Then, the change of the input voltages $U_{\text{in}X}$ will not be the same as the requirement. Therefore, in terms of adjusting the input voltages for each DAB module, the coupling of the regulation of the input voltages and the adjustment of the output voltage cannot be neglected.

III. Proposed Input-Oriented Power Sharing Control Scheme With Fast-Dynamic Response

In this section, the novel input-oriented power sharing control scheme with fast-dynamic response will be proposed for the ISOP DAB dc–dc converter. To reduce the power loss, an existing MCS modulation method is adopted [30]. Then, the proposed power sharing control scheme will be presented and analyzed, which can also provide fast-dynamic response when the input voltage and load resistor are changed.

A. Minimum-Current-Stress Modulation Method

The waveforms of the MCS modulation method can be shown in Fig. 4, where D_{X1}–D_{X3} are the phase-shift ratios. Based on

TABLE I
OPTIMIZED SOLUTIONS OF MCSO STRATEGY UNDER DIFFERENT CONDITIONS

Voltage Conditions	Unified Transferred Current	Range of i_{TX}	Middle Variable	Phase-Shift Ratio
$k>1$	$i_{TX}=\frac{8L_XI_{TX}}{n_XU_{inX}T_s}$	$0\le i_{TX}<2\frac{k_X-1}{k_X^2}$	$D_{X1}=1-\sqrt{\frac{i_{TX}}{2(k_X-1)}}$	$\begin{cases}D_{X2}=(k_X-1)(1-D_{X1})\\D_{X3}=D_{X1}\end{cases}$
		$2\frac{k_X-1}{k_X^2}\le i_{TX}\le 1$	$D_{X1}=(k_X-1)\sqrt{\frac{1-i_{TX}}{k_X^2-2k_X+2}}$	$\begin{cases}D_{X2}=\frac{k_X-2}{2(k_X-1)}D_{X1}+\frac{1}{2}\\D_{X3}=\frac{k_X-2}{2(k_X-1)}D_{X1}+\frac{1}{2}\end{cases}$
$k\le 1$		$0\le i_{TX}<2(k_X-k_X^2)$	$D_{X1}=1-\sqrt{\frac{i_{TX}}{2k_X(1-k_X)}}$	$\begin{cases}D_{X2}=0\\D_{X3}=k_XD_{X1}-k_X+1\end{cases}$
		$2(k_X-k_X^2)\le i_{TX}\le 1$	$D_{X2}=\frac{1}{2}(1-\sqrt{\frac{1-i_{TX}}{2k_X^2-2k_X+1}})$	$\begin{cases}D_{X1}=0\\D_{X3}=2k_XD_{X2}\text{-}D_{X2}-k_X+1\end{cases}$

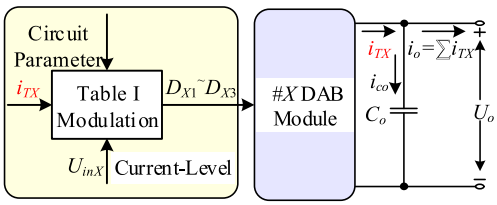

Fig. 5. Schematic of current-level modulation for the DAB dc–dc converter.

this modulation method, the soft switching performance can be obtained during the whole power range, and the minimum conduction power loss can also be achieved. Then, the corresponding phase-shift ratios D_{X1}–D_{X3} can be given from Table I, where I_{TX} is the transferred current, n_X is the transformer turn ratio, k_X is the voltage ratio as n_XU_{inX}/U_o, and L is the middle inductance of the Xth DAB dc–dc module.

Compared with Fig. 3 and Table I, the transferred current I_{TX} can be expressed as

$$I_{TX}=\frac{i_{\text{in}X}U_{\text{in}X}}{U_o}. \tag{11}$$

Moreover, based on Table I, the current-level modulation operation can be realized, and the corresponding schematic can be shown in Fig. 5.

As shown in Fig. 5, if the transferred current I_{TX} is employed as the effective control value for the DAB dc–dc converter, the current-level modulation can be employed. Based on some existing modulation methods [30], the phase-shift ratios can be determined by the transferred current or power even during the transient process. Then, when the DAB converter is modeled, the underlying phase-shift ratios can be avoided, which can significantly simplify the modeling analysis about the DAB converter.

B. Proposed Input-Oriented Power Sharing Control Method With Fast-Dynamic Response

According to (10), when the input voltages should be controlled positively, the influence on the output voltage is unavoidable. So, to reduce this influence, the changes $\Delta U_{\text{in}X}$ of each input voltage should be relatively small. Then, the charging current $i_{\text{cin}X}$ for each input-side capacitor can be calculated as

$$i_{\text{cin}X}=\frac{\Delta U_{\text{in}X}C_{\text{in}X}}{T_s}. \tag{12}$$

Moreover, to deal with the disturbance of the load condition, the required output current for the ISOP DAB dc–dc converter can be calculated as

$$i_o^*=\frac{U_o^*}{R_{\text{eq}}}=\frac{i_oU_o^*}{U_o} \tag{13}$$

where U^*_o is the desired output voltage and R_{eq} is the equivalent load resistor. Since the power losses cannot be neglected in the actual converter system, a compensation value k_c should be introduced by using the fuzzy adjustment of the PI controller. The compensation value k_c can be the output value of the PI controller with the output voltage and its desired value as inputs. Then, the static error can be reduced, and (13) can be further expressed as

$$i_o^*=k_c\frac{i_oU_o^*}{U_o}. \tag{14}$$

In (14), all DAB modules should share this required output current i^*_o. Traditionally, the existing strategies prefer to divide this required output current evenly for each dc–dc converter module [15], [16], [19], [26], and [27]. However, this operation will usually influence the regulation of the input voltages since the DAB modules have different transferred current abilities with different input voltages, and the input-side capacitors have to compensate for the transferred currents. Then, the adjustment of the output voltage will influence the input voltages when the input voltages are not the same. To meet the current transferred abilities of each DAB module, the transferred current i_{TX} for meeting the requirement of the output side should be expressed as

$$i_{TX}=\frac{i_o^*U_{\text{in}X}}{U_{\text{in}}}. \tag{15}$$

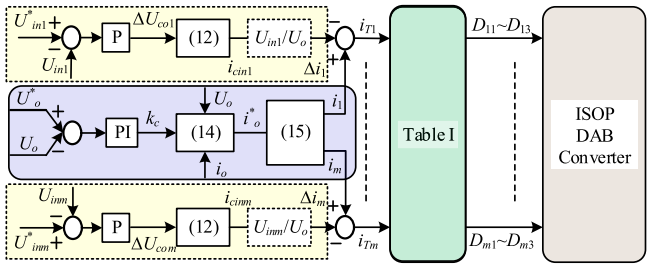

Fig. 6. Diagram of the proposed input-oriented power sharing control scheme with fast dynamic response for ISOP DAB dc–dc converter.

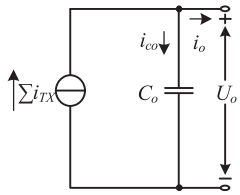

Fig. 7. Simplified circuit of the ISOP DAB dc–dc converter.

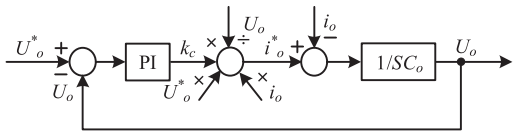

Fig. 8. Control schematic for regulating the output voltage.

According to (15), when the input voltage and the load condition are changed, the influence on the voltage sharing performance on the input side can be significantly eliminated. Then, combining Table I, (12), (14), and (15), the proposed input-oriented power sharing control scheme with fast-dynamic response can be demonstrated in Fig. 6. At the beginning of the switching period, the input voltages, the output voltage, and the load current are measured. Based on the error of the output voltage and its desired value, the compensated value k_c can be obtained from the PI controller. Then, according to (14), the required output current can be calculated based on (15), the required transferred current i_X of each DAB module for meeting the requirement of load side can be obtained. Moreover, based on the error of the input voltages and their desired values, the required change values for each input voltage can be obtained based on a proportionality controller. Then, according to (12) and $U_{\mathrm{in}X}/U_o$, the required transferred current Δi_X for adjusting the input voltages can be obtained. However, since the input voltages of each module may be very different, the item $U_{\mathrm{in}X}/U_o$ will usually result in large difference of transferred currents for charging and discharging the input-side capacitors. So, it is better to delete this item in the control system. Furthermore, the total required transferred current I_{TX} can be calculated as the difference of i_X and Δi_X. Finally, based on Table I, the corresponding phase-shift ratios can be obtained, and the proposed strategy can be implemented for positively adjusting the input voltages and dealing with the disturbance of the total input voltage and the load condition.

C. Designs of the P Parameter and the PI Parameters in the Proposed Scheme

Combining (8), (10), and Fig. 6, when the input voltages of the DAB modules are adjusted, the disturbance of the output voltage ΔU_o in a switching period can be expressed as

$$\Delta U_o = \sum_{X=1}^{m} \frac{\Delta i_{\mathrm{in}X} U_{\mathrm{in}X} T_s}{C_o U_o} = \frac{\sum_{X=1}^{m} k_{p\mathrm{in}} (U^*_{\mathrm{in}X} - U_{\mathrm{in}X}) C_X U_{\mathrm{in}X} T_s}{C_o U_o} \tag{16}$$

where $k_{p\mathrm{in}}$ is the proportional parameter of the P controller. Then, assuming the allowable output-voltage disturbance

TABLE II
CIRCUIT PARAMETERS OF THE ISOP DAB DC–DC CONVERTER SYSTEM

L_1, L_2	40μH
n_1, n_2	1
f_s	40 kHz
R	15Ω ~ 50Ω
U_{in}	100V ~120V
U^*_o	50V
k_p, k_i, k_{Pin}	0.05, 0.005, 0.2
C_{in1}, C_{in2}, C_o	1mF

$\Delta U_{o\max}$, $k_{p\mathrm{in}}$ can be calculated as

$$k_{p\mathrm{in}} \le \frac{C_o U_o \Delta U_o}{\sum_{X=1}^{m} (U^*_{\mathrm{in}X} - U_{\mathrm{in}X}) C_X U_{\mathrm{in}X} T_s}. \tag{17}$$

Moreover, since storage energy in middle inductance at the beginning and the end of a switching period can be regarded as the same at the steady-state condition and during the transient process, the simplified circuit of the ISOP DAB dc–dc converter can be shown in Fig. 7.

To reduce the influence on the output voltage during the adjustment of the input voltages, the variations of the input-capacitor currents should be very small. Thus, these branches for adjusting the input voltages can be eliminated when analyzing the PI parameters of the middle PI controller in Fig. 6. Then, the control schematic for regulating the output voltage can be demonstrated in Fig. 8.

According to Fig. 8, the transfer function with control-loop delay can be expressed as

$$H(s) = \frac{U^*_o i_o}{U_o} \frac{k_p s + k_i}{s} \frac{1}{sC_o} e^{-T_s}. \tag{18}$$

In addition, the main circuit parameters of the ISOP DAB dc–dc converter can be shown in Table II. Combining (18), the bode diagram can be demonstrated as Fig. 9.

As shown in Fig. 9, the measured simulation frequency response results are similar to the bode diagram, and the phase margin at cross-over frequency is bigger than 45° as 90°. Therefore, the stability of the proposed power sharing control scheme

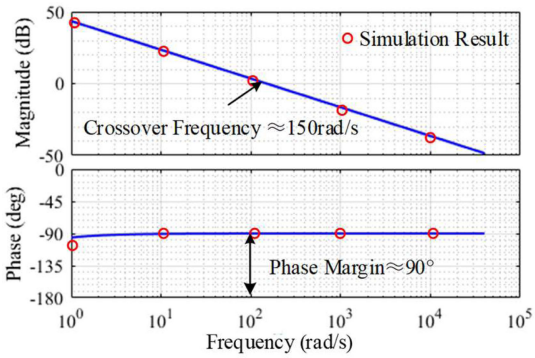

Fig. 9. Bode diagram of control loop for regulating the output voltage.

with fast-dynamic response can be ensured for the ISOP DAB dc–dc converter.

Moreover, by using the parameters at rating condition, the close-loop transfer function of the proposed scheme for the ISOP DAB dc–dc converter can be expressed as

$$G(s) = \frac{500se^{-T_s} + 50e^{-T_s}}{3s^2 + 500se^{-T_s} + 50e^{-T_s}}. \tag{19}$$

According to (19), the poles of the close-loop transfer function can be calculated as

$$P(s) = \frac{-500e^{-T_s} \pm \sqrt{(500e^{-T_s})^2 - 600e^{-T_s}}}{6} < 0. \tag{20}$$

Therefore, (20) can furtherly verify the stability of the proposed scheme for the ISOP DAB dc–dc converter.

D. Inductance-Estimating Method for Ensuring the Desired Power Sharing Performance

According to Table I, the circuit parameters are employed to realize the power sharing performance of the ISOP DAB dc–dc converter system. So, if the employed inductance is not accurate, the power sharing performance should be affected without the integral function for adjusting the input voltages. When the steady-state condition is achieved, the relationship between the input power and the output power for each DAB module can be expressed as

$$\begin{aligned} &i_{\text{in}}U_{\text{in}1} : \ldots i_{\text{in}}U_{inX} : \ldots i_{\text{in}}U_{\text{in}m} \\ &= i'_{T1}U_o : \ldots i'_{TX}U_o : \ldots i'_{Tm}U_o \end{aligned} \tag{21}$$

where i'_{TX} is the actual transferred power for each DAB module. Assuming the actual inductance for each DAB module is L'_X, (21) can be further expressed as

$$U_{in1} : \ldots U_{\text{in}X} : \ldots U_{\text{in}m} = \frac{i_{T1}L_1}{L'_1} : \ldots \frac{i_{TX}L_X}{L'_X} : \frac{i_{Tm}L_m}{L'_m}. \tag{22}$$

Then, by using the first inductance L'_1 as a reference, the other inductance can be calculated as

$$L'_X = \frac{i_{TX}L_XL'_1U_{\text{in}1}}{i_{T1}L_1U_{\text{in}X}}. \tag{23}$$

According to (23), the total transferred current i_T can be calculated as

$$i_T = \frac{i_{T1}L_1}{L'_1} + \sum_{X=2}^{m} \frac{i_{T1}L_1U_{\text{in}X}}{L'_1U_{\text{in}1}}. \tag{24}$$

Based on the Law of Conservation of Energy, the total transferred current i_T should be equivalent to the desired output current i^*_o as

$$i_T = i^*_o = \frac{i_{T1}L_1}{L'_1} + \sum_{\alpha=2}^{m} \frac{i_{T1}L_1U_{\text{in}X}}{L'_1U_{\text{in}1}}. \tag{25}$$

According to (25), the actual inductance L'_1 of the first DAB module can be expressed as

$$L'_1 = \frac{i_{T1}L_1}{i^*_o} + \sum_{X=2}^{m} \frac{i_{T1}L_1U_{\text{in}X}}{i^*_oU_{\text{in}1}}. \tag{26}$$

Then, combining (23), the inductances of other DAB modules can be estimated. Sometimes, the inductance values of the ISOP DAB dc–dc converter system may be unknown, a general inductance-estimating method will be presented as follow. For each DAB converter, the transferred current can be expressed by the calculated phase-shift ratios as [8]

$$i_{TX} = \frac{U_{\text{in}X}f(D_{X1}, D_{X2}, D_{X3})T_s}{4n_XL_X}. \tag{27}$$

Combining (15) and (27), the estimated inductance for each DAB module can be expressed as

$$L'_X = \frac{f(D_{X1}, D_{X2}, D_{X3})U_{\text{in}}T_s}{4i^*_on_X}. \tag{28}$$

According to (28), the preset inductance can be eliminated. So, even without knowledge of inductance values, the presented general inductance-estimating method can be employed in other control schemes with the measurement of load current for the ISOP DAB dc–dc converter system. Moreover, since the inductance-estimating method should be employed in the steady-state condition for a more accurate estimated value, the decoupling between the estimating process and the transient process should be realized, especially for dealing with the load-resistor disturbance. To deal with this issue, the change of the load current can be employed to stop the estimating process, and the change of the input voltage should be observed for ensuring the steady-state condition of input voltages. Then, when the change of the input voltage in two continuous switching periods is smaller than the peak value of the measurement noise, the estimating operation can be activated again. The time duration of these two switching periods should be big enough such as more than half of the change time of the input voltages.

IV. Verification

In this section, based on the circuit parameters in Table II, a simulation model and a small-scale experimental platform with two DAB modules are built to verify effectiveness of the proposed input-oriented power sharing control method with fast-dynamic response for the ISOP DAB dc–dc converter system.

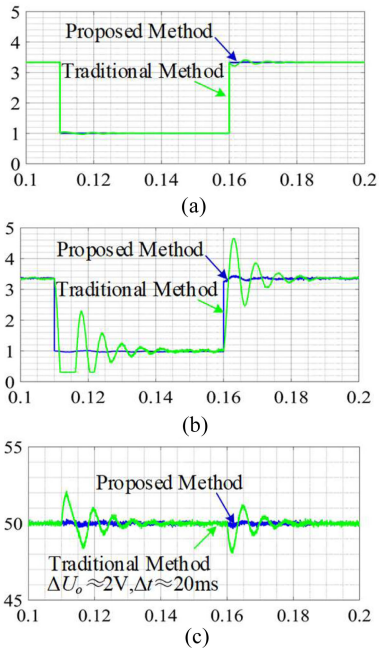

Fig. 10. Simulation results when the load resistor is changed (*t*: 20 ms/div). (a) Load current (A). (b) Total transferred current (A). (c) Output voltage (V).

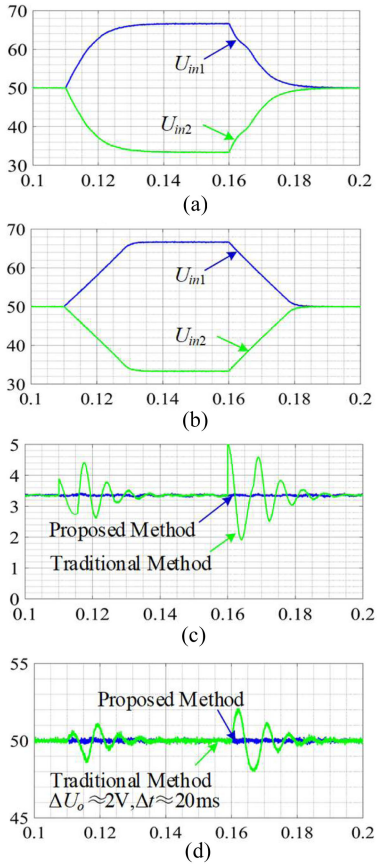

Fig. 11. Simulation results when the power sharing performance is changed (*t*: 20 ms/div). (a) Input voltage (V) under the traditional method. (b) Input voltage(V) under the proposed method. (c) Total transferred current (A). (d) Output voltage (V).

A. Simulation Results

In the simulation part, the comparison of the traditional method [26], [27] and the proposed input-oriented power sharing control scheme with fast-dynamic response will be provided. Moreover, by using the proposed general inductance-estimating method for the ISOP DAB dc–dc converter, the inductance values under the traditional method are estimated with the measurement of the load current.

When the input voltage is 100 V and the power balance performance is achieved, Fig. 10 shows the simulation results of the traditional method and the proposed scheme when the load resistor is changed between 15 and 50 Ω. As shown in Fig. 10(b), when the load resistor is changed, the total transferred current Σi_{TX} under the proposed scheme can follow with the change of the load current timely as shown in Fig. 10(a). Thus, as shown in Fig. 10(c), the output voltage can remain at its desired value 50 V by using the proposed scheme. However, compared with Fig. 10(a) and (b) under the traditional method, the total transferred current can not be stable at the required current timely, so the output voltage disturbances are obvious.

Moreover, when the input voltage is 100 V and the load resistor is 15 Ω, Fig. 11 shows the simulation results when the power sharing performance of these two DAB modules is changed between 1:1 and 2:1 [see from Fig. 11(a) and (b)]. As shown in Fig. 11(c), during the regulation of input voltages, the transferred current under the proposed scheme can keep constant, but the transferred current under the traditional method has some disturbances. Then, according to Fig. 11(d), the stable output voltage can be obtained by using the proposed scheme, but the output-voltage disturbances under the traditional method are obvious.

In addition, when L_1 is changed to 30 μH in the simulation model, Fig. 12 shows the simulation results of the proposed inductance-estimating method embedded in the traditional method [26], [27] at the cost of an additional load-current sensor. As shown in Fig. 12(a), the estimated inductances are close to the setup values. The relationship of these two estimated inductances can be accurate as shown in Fig. 12(b). Therefore, the proposed general inductance-estimating method can also be employed in other control schemes for the ISOP DAB dc–dc converter if the accuracy of the inductances should be ensured.

B. Experimental Results

When the inductance of the first DAB module L_1 is inaccurate as 24 μH, Fig. 13 shows the experimental results when the input voltage and the load resistor are changed. As shown in Fig. 13(a) and (b), when the total input voltage is changed between 100 and 120 V, the output voltage U_o can be kept at its desired value as 50 V. However, the power balance performance cannot be achieved since the inductance value L_1 is not accurate. Moreover, as shown in Fig. 13(c) and (d), when the load resistor is changed between 15 and 50 Ω, the output voltage U_o can be stable at its desired value. Therefore, when the inductance value is not accurate, the desired power sharing performance cannot be

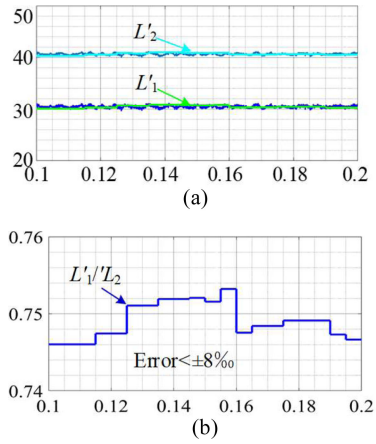

Fig. 12. Simulation results of the estimated inductance by using the proposed general inductance-estimating method embedded in the traditional control method (t: 20 ms/div). (a) Estimated inductances (μH). (b) Relationship of L'_1 and L'_2.

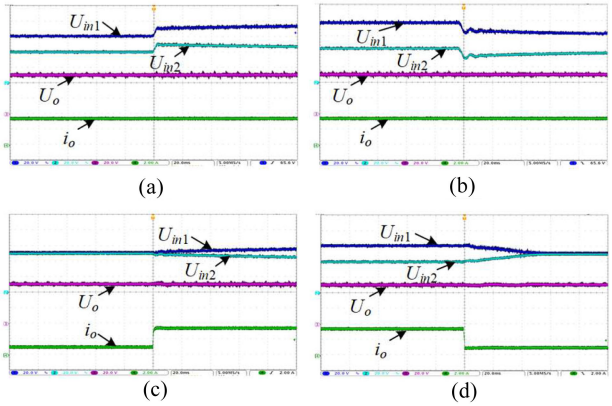

Fig. 13. Experimental results when $L_1 = 24\ \mu$H and $L_2 = 40\ \mu$H ($U_{\rm in1}$, $U_{\rm in2}$ and U_o: 20 V/div; i_o: 2 A/div; and t: 20 ms/div). (a) U_{in} : 100 $V \rightarrow$ 120 V. (b) U_{in} : 120 $V \rightarrow$ 100 V. (c) R : 50 $\Omega \rightarrow$ 15 Ω. (d) R : 15 $\Omega \rightarrow$ 50 Ω.

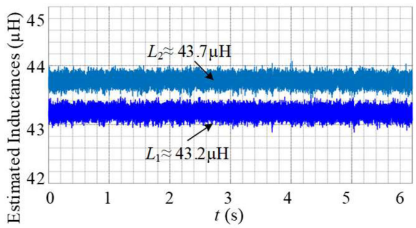

Fig. 14. Estimated inductances.

realized, but the excellent dynamic response can be provided for the ISOP DAB dc–dc converter.

Then, when the total input voltage is 100 V, the desired output voltage is 50 V and the load resistor is 15 Ω, the experiment result of these estimated inductances of these two DAB modules can be shown in Fig. 14. As shown in Fig. 14, the estimated inductance of the first DAB module L_1 is 43.2 μH, and the estimated inductance of the second DAB module L_2 is 43.7 μH. Thus, these estimated inductances are close to the actual inductances

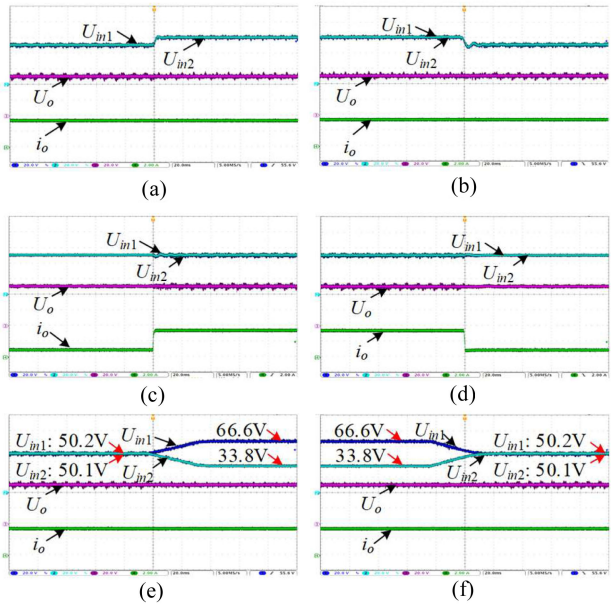

Fig. 15. Experimental results with estimated inductances $L_1 = 43.2\ \mu$H and $L_2 = 43.7\ \mu$H ($U_{\rm in1}$, $U_{\rm in2}$ and U_o: 20 V/div; i_o: 2 A/div; and t: 20 ms/div). (a) U_{in} : 100 $V \rightarrow$ 120 V. (b) U_{in} : 120 $V \rightarrow$ 100 V. (c) R : 50 $\Omega \rightarrow$ 15 Ω. (d) R : 15 $\Omega \rightarrow$ 50 Ω. (e) $P_1 : P_2 = (1:1) \rightarrow (2:1)$. (d) $P_1 : P_2 = (2:1) \rightarrow (1:1)$.

as given in Table II but a little bigger, which should be caused by the power losses.

Based on the estimated inductances, the experiment results can be shown in Fig. 15 when the input voltage, the load resistor, and the power sharing performance are changed. A shown in Fig. 15(a) and (b), the power balance performance of the ISOP DAB dc–dc converter can be ensured, and when the input voltage is changed, the output voltage can be stable at its desired value. Moreover, as shown in Fig. 15(c) and (d), when the load resistor is changed between 15 and 50 Ω, the output-voltage disturbance can be regarded as zero. In addition, As shown in Fig. 15(e) and (f), when the desired power sharing performance of these two DAB modules is changed between 1:1 and 2:1, the corresponding actual power sharing performances are 1:1 and 1.97:1. So, based on the proposed scheme, the power sharing performance of the ISOP DAB dc–dc converter can be adjusted flexibly. Furthermore, when the power sharing performance is changed, the output voltage can be kept at its desired value. Therefore, with the estimated inductances, the required power sharing performance can be ensured, and an excellent dynamic response can be achieved when the input voltage, the load resistor, and the power sharing performance are changed.

With the actual inductances of these two DAB modules, the experiment results, when the input voltage, the load resistor, and the power sharing performance are changed, can be shown in Fig. 16. Similarly, when the input voltage, the load resistor, and the power sharing performance of the ISOP DAB dc–dc converter are changed, the output voltage can be kept at its desired value, and the excellent dynamic performance can be provided for this converter system. Moreover, as shown in Fig. 16(e) and

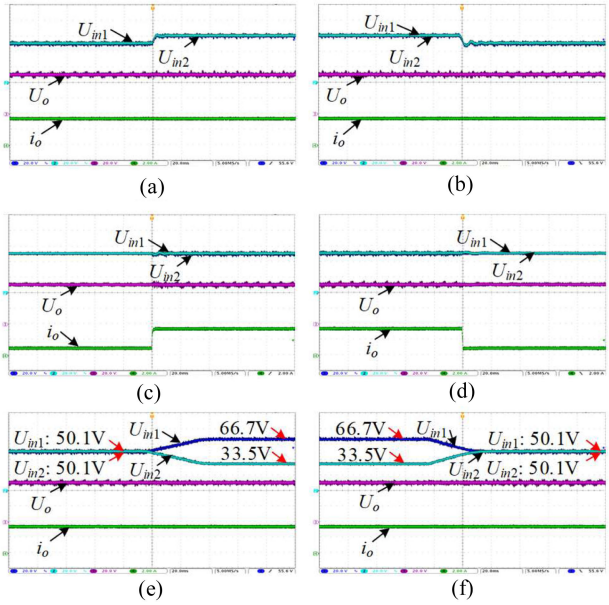

Fig. 16. Experimental results when $L_1 = 40\ \mu$H and $L_2 = 40\ \mu$H (U_{in1}, U_{in2} and U_o: 20 V/div; i_o: 2 A/div; and t: 20 ms/div). (a) U_{in} : 100 $V \rightarrow$ 120 V. (b) U_{in} : 120 $V \rightarrow$ 100 V. (c) $R : 50\ \Omega \rightarrow 15\ \Omega$. (d) $R : 15\ \Omega \rightarrow 50\ \Omega$. (e) $P_1 : P_2 = (1 : 1) \rightarrow (2 : 1)$. (f) $P_1 : P_2 = (2 : 1) \rightarrow (1 : 1)$.

(f), when the desired output power of the first DAB module is double as that of the second DAB module, the actual power sharing performance of these two modules is 1.99: 1, and when the desired output power of the first DAB modules should be the same as that of the second DAB module, this power balance requirement can be achieved. Therefore, with actual inductance values, the desired power sharing performance can be ensured for the ISOP DAB dc–dc converter by using the proposed input-oriented power sharing control scheme with fast-dynamic response. Thus, experiment results in Fig. 16 can be a reference for experiment results in Fig. 15, which can be employed to verify the effectiveness of the proposed inductance-estimating method.

V. Conclusion

In this article, an input-oriented power sharing control scheme with fast-dynamic response is proposed for the ISOP DAB dc–dc converter system. With the average model of this converter system, the coupling between adjusting power sharing performance and maintaining the output voltage is analyzed. Based on the proposed scheme, this coupling can be reduced significantly. Moreover, the proposed scheme can provide the excellent dynamic response for the DAB dc–dc converter, and the robustness of the converter system can be enhanced markedly. The conducted studies are summarized as follows.

1) The coupling between adjusting power sharing performance and maintaining the output voltage of the ISOP DAB dc–dc converter is unavoidable. Then, during the adjusting of the power sharing performance, the total transferred current caused by the regulation of the input voltages should be controlled close to zero, or the regulation of the input voltages should be slow enough. Then, the influence on the output voltage can be reduced significantly.
2) When the adopted inductance value of the ISOP DAB dc–dc converter is inaccurate, the power sharing performance of this converter system will be damaged. Under this condition, the excellent dynamic response of output voltage can also be obtained by using the proposed scheme.
3) Based on the proposed inductance-estimating method, the inductance values for each DAB module can be estimated, which can be employed to ensure the power sharing performance of the ISOP DAB dc–dc converter system. Moreover, the proposed inductance-estimating method can be embedded in other control schemes for these DAB-based converter systems if the accuracy of inductances is required.
4) Based on the proposed input-oriented power sharing control strategy with fast-dynamic response, the excellent dynamic response can be provided for the ISOP DAB dc–dc converter when the total input voltage, the load resistor, and the power sharing performance are changed.

References

[1] J.-W. Kim, J.-S. Yon, and B. H. Cho, "Modeling, control, and design of input-series-output-parallel-connected converter for high-speed-train power system," *IEEE Trans. Ind. Electron.*, vol. 48, no. 3, pp. 536–544, Jun. 2001.

[2] J. Duan, D. Zhang, L. Wang, Z. Zhou, and Y. Gu, "Active voltage sharing module for input-series connected modular DC/DC converters," *IEEE Trans. Power Electron.*, vol. 35, no. 6, pp. 5987–6000, Jun. 2020.

[3] J. Liu, J. Yang, J. Zhang, Z. Nan, and Q. Zheng, "Voltage balance control based on dual active bridge DC/DC converters in a power electronic traction transformer," *IEEE Trans. Power Electron.*, vol. 33, no. 2, pp. 1696–1714, Feb. 2018.

[4] D. Ma, W. Chen, and X. Ruan, "A review of voltage/current sharing techniques for series–parallel-connected modular power conversion systems," *IEEE Trans. Power Electron.*, vol. 35, no. 11, pp. 12383–12400, Nov. 2020.

[5] J. Xu *et al.*, "High-speed electromagnetic transient (EMT) equivalent modelling of power electronic transformers," *IEEE Trans. Power Del.*, vol. 36, no. 2, pp. 975–986, Apr. 2021.

[6] G. Daoud, E. Hassan Aboadla, S. Khan, S. Faiz Ahmed, and M. Tohtayong, "Input-series output-parallel full-bridge DC-DC converter for high power applications," in *Proc. 4th IEEE Int. Conf. Eng. Technol. Appl. Sci.*, 2017, pp. 1–6.

[7] C. Gammeter, F. Krismer, and J. W. Kolar, "Comprehensive conceptualization, design, and experimental verification of a weight-optimized All-SiC 2 kV/700 V DAB for an airborne wind turbine," *IEEE J. Emerg. Sel. Topics Power Electron.*, vol. 4, no. 2, pp. 638–656, Jun. 2016.

[8] N. Hou and Y. W. Li, "Overview and comparison of modulation and control strategies for a nonresonant single-phase dual-active-bridge DC–DC converter," *IEEE Trans. Power Electron.*, vol. 35, no. 3, pp. 3148–3172, Mar. 2020.

[9] R. W. A. A. De Doncker, D. M. Divan, and M. H. Kheraluwala, "A three-phase soft-switched high-power-density DC/DC converter for high-power applications," *IEEE Trans. Ind. Appl.*, vol. 27, no. 1, pp. 63–73, Jan./Feb. 1991.

[10] W. Chen, X. Ruan, H. Yan, and C. K. Tse, "DC/DC conversion systems consisting of multiple converter modules: Stability, control, and experimental verifications," *IEEE Trans. Power Electron.*, vol. 24, no. 6, pp. 1463–1474, Jun. 2009.

[11] R. Giri, V. Choudhary, R. Ayyanar, and N. Mohan, "Common-duty-ratio control of input-series connected modular DC-DC converters with active input voltage and load-current sharing," *IEEE Trans. Ind. Appl.*, vol. 42, no. 4, pp. 1101–1111, Jul./Aug. 2006.

[12] D. Ochoa, A. Barrado, A. Lázaro, R. Vázquez, and M. Sanz, "Modeling, control and analysis of input-series-output-parallel-output-series architecture with common-duty-ratio and input filter," in *Proc. IEEE 19th Workshop Control Model. Power Electron.*, 2018, pp. 1–6.

[13] J. Shi, J. Luo, and X. He, "Common-duty-ratio control of input-series output-parallel connected phase-shift full-bridge DC–DC converter modules," *IEEE Trans. Power Electron.*, vol. 26, no. 11, pp. 3318–3329, Nov. 2011.
[14] J. Shi, L. Zhou, and X. He, "Common-duty-ratio control of input-parallel output-parallel (IPOP) connected DC–DC converter modules with automatic sharing of currents," *IEEE Trans. Power Electron.*, vol. 27, no. 7, pp. 3277–3291, Jul. 2012.
[15] J. W. Kimball, J. T. Mossoba, and P. T. Krein, "A stabilizing, high-performance controller for input series-output parallel converters," *IEEE Trans. Power Electron.*, vol. 23, no. 3, pp. 1416–1427, May 2008.
[16] M. Abrehdari and Mohammad Sarvi, "Comprehensive sharing control strategy for input-series output-parallel connected modular DC–DC converters," *IET Power Electron.*, vol. 12 no. 12, pp. 3105–3117, 2019.
[17] W. Chen, X. Zhu, G. Wang, W. Jiang, and K. Yao, "A novel input voltage sharing control strategy for input-series output-parallel system with high reliability," in *Proc. IEEE Energy Convers. Congr. Expo.*, 2014, pp. 1207–1212.
[18] R. Ding, F. Wang, N. Zhang, S. Shi, S. Cheng, and F. Zhuo, "A decentralized control strategy with output voltage deviation-correction for input-series-output-parallel DC transformer based on dual-active-bridge," in *Proc. IEEE 9th Int. Power Electron. Motion Control Conf.*, 2020, pp. 2458–2462.
[19] L. Qu, D. Zhang, and Z. Bao, "Output current-differential control scheme for input-series–output-parallel-connected modular DC–DC converters," *IEEE Trans. Power Electron.*, vol. 32, no. 7, pp. 5699–5711, Jul. 2017.
[20] P. J. Grbovic, "Master/slave control of input-series- and output-parallel-connected converters: Concept for low-cost high-voltage auxiliary power supplies," *IEEE Trans. Power Electron.*, vol. 24, no. 2, pp. 316–328, Feb. 2009.
[21] D. Sha, Z. Guo, and X. Liao, "Cross-feedback output-current-sharing control for input-series-output-parallel modular DC–DC converters," *IEEE Trans. Power Electron.*, vol. 25, no. 11, pp. 2762–2771, Nov. 2010.
[22] S. H. Kim, B. J. Kim, and C. Y. Won, "A study on decentralized inverse-droop control for input voltage sharing of ISOP converter in the current control loop," in *Proc. 10th Int. Conf. Power Electron. ECCE Asia*, 2019, pp. 2382–2387.
[23] G. Xu, D. Sha, and X. Liao, "Decentralized inverse-droop control for input-series–output-parallel DC–DC converters," *IEEE Trans. Power Electron.*, vol. 30, no. 9, pp. 4621–4625, Sep. 2015.
[24] Y. Huang, C. K. Tse, and X. Ruan, "General control considerations for input-series connected DC/DC converters," *IEEE Trans. Circuits Syst. I, Reg. Papers*, vol. 56, no. 6, pp. 1286–1296, Jun. 2009.
[25] L. Qu and D. Zhang, "Input voltage sharing control scheme for input series and output series DC/DC converters using paralleled MOSFETs," *IET Power Electron.*, vol. 11 no. 2, pp. 382–390, 2017.
[26] P. Zumel *et al.*, "Modular dual-active bridge converter architecture," *IEEE Trans. Ind. Appl.*, vol. 52, no. 3, pp. 2444–2455, May/Jun. 2016.
[27] C. Luo and S. Huang, "Novel voltage balancing control strategy for dual-active-bridge input-series-output-parallel DC-DC converters," *IEEE Access*, vol. 8, pp. 103114–103123, 2020.
[28] W. Song, N. Hou, and M. Wu, "Virtual direct power control scheme of dual active bridge DC–DC converters for fast dynamic response," *IEEE Trans. Power Electron.*, vol. 33, no. 2, pp. 1750–1759, Feb. 2018.
[29] V. M. Iyer, S. Gulur, and S. Bhattacharya, "Small-signal stability assessment and active stabilization of a bidirectional battery charger," *IEEE Trans. Ind. Appl.*, vol. 55, no. 1, pp. 563–574, Jan./Feb. 2019.
[30] N. Hou, W. Song, and M. Wu, "Minimum-current-stress scheme of dual active bridge DC–DC converter with unified phase-shift control," *IEEE Trans. Power Electron.*, vol. 31, no. 12, pp. 8552–8561, Dec. 2016.

Nie Hou (Student Member, IEEE) received the B.S. and M.S. degrees in electrical engineering from Southwest Jiaotong University, Chengdu, China, in 2014 and 2017, respectively. He is currently working toward the Ph.D. degree with the Department of Electrical and Computer Engineering, University of Alberta, Edmonton, AB, Canada.

His current research interests include digital control and optimization methods of dc–dc converter and dc distribution system.

Mr. Hou was the recipient of the Outstanding Author Award from the Proceeding of the Chinese Society for Electrical Engineering in 2016 and the Second Prize of IAS Sustainable and Renewable Energy Conversion System Committee Conference Paper Awards in 2021.

Pasan Gunawardena (Student Member, IEEE) received the B.Sc. degree in electrical engineering and the M.Phil. degree in electronics and telecommunication engineering from the University of Moratuwa, Moratuwa, Sri Lanka, in 2015 and 2019, respectively. He is currently working toward the Ph.D. degree in energy systems with the Department of Electrical and Computer Engineering, University of Alberta, Edmonton, AB, Canada.

His current research interests include dc–dc converter topologies and dc microgrid systems.

Mr. Gunawardena was the recipient of the Second Prize of the IAS Renewable and Sustainable Energy Conversion Systems Committee Conference Paper Awards in 2021.

Xuesong Wu (Student Member, IEEE) received the B.Eng. (Yisheng Mao Hons.) and M.Sc. degree electrical engineering from Southwest Jiaotong University, Chengdu, China, in 2016 and 2019, respectively. He is currently working toward the Ph.D. degree with the Department of Electrical and Computer Engineering, University of Alberta, Edmonton, AB, Canada.

His research interests include the electrical machine drives and grid-tied inverters.

Li Ding (Member, IEEE) received the B.Eng. degree from Shanghai University, Shanghai, China, in 2013, the M.Sc. degree from the Harbin Institute of Technology, Harbin, China, in 2015, and the Ph.D. degree from the University of Alberta, Edmonton, AB, Canada, in 2020, all in electrical engineering.

He is currently working as a Postdoctoral Research Fellow with the Department of Electrical and Computer Engineering, University of Alberta, Edmonton, AB, Canada. His research interests include current-source converters, sensorless motor drives, multilevel converters, wide band-gap devices, and parameter identification.

Yue Zhang (Member, IEEE) received the B.Sc. and M.Sc. degrees from the Nanjing University of Aeronautics and Astronautics, Nanjing, China, in 2012 and 2015, and the Ph.D. degree from Southeast University, Nanjing, China, in 2020, all in electrical engineering.

From 2017 to 2019, he was a Visiting Ph.D. Student with the University of Alberta, Edmonton, AB, Canada, where he is currently a Postdoctoral Fellow. His research interests include dc/dc converters and magnetic design.

Yun Wei Li (Fellow, IEEE) received the B.Sc.Eng. degree in electrical engineering from Tianjin University, Tianjin, China, in 2002, and the Ph.D. degree from Nanyang Technological University, Singapore, in 2006.

In 2005, he was a Visiting Scholar with Aalborg University, Aalborg, Denmark. From 2006 to 2007, he was a Postdoctoral Research Fellow with Ryerson University, Toronto, ON, Canada. In 2007, he was with Rockwell Automation Canada before he joined the University of Alberta. Since then, he has been with the University of Alberta, where he is currently a Professor. His research interests include distributed generation, microgrid, renewable energy, high power converters, and electric motor drives.

Dr. Li is currently the Editor-in-Chief for the IEEE TRANSACTIONS ON POWER ELECTRONICS LETTERS. Prior to that, he was an Associate Editor for the IEEE TRANSACTIONS ON POWER ELECTRONICS, IEEE TRANSACTIONS ON INDUSTRIAL ELECTRONICS, IEEE TRANSACTIONS ON SMART GRID, and IEEE JOURNAL OF EMERGING AND SELECTED TOPICS IN POWER ELECTRONICS. He was the General Chair of IEEE Energy Conversion Congress of Exposition in 2020. He was the recipient of the Richard M. Bass Outstanding Young Power Electronics Engineer Award from IEEE Power Electronics Society in 2013, the IEEE Northern Canada Outstanding Engineer Award in 2016, as well as four Paper Awards. He is recognized as a Highly Cited Researcher by the Web of Science Group.